4.4 Cavity Design Options

The cavity environment is very severe for an IFE reactor. Not only is the time-averaged neutron fluence similar to that of an MFE reactor, the pulsed nature of IFE adds blast effects, instantaneous high heat loads, and high levels of X ray and gamma radiation. A large number of IFE cavity design studies have been performed during the past ten years. The selection of a cavity concept for Prometheus was preceded by a thorough review of existing designs. The trade studies for the wall protection and the blanket are described in the following sections.

4.4.1 Wall Protection Concept - The protection of the wall is one the most critical engineering challenges in the reactor plant. The adverse environment is very harsh because of the pulsed nature of the inertial fusion reaction. A majority of the energy release occurs almost instantaneously in the form of prompt X rays, neutrons, and photons. The debris ions provide the remainder of the energy deposition a short time later. After the initial energy release, the cavity chamber is "relatively quiescent" which allows the environment and chamber wall/structure to equilibrate, thermally and mechanically. This process
is repeated many times a second and hundreds of millions of times per year which imposes a daunting fatigue challenge to design and manufacture a reliable and long-lived first wall system.

4.4.1.1 Wall Protection Design Options – The major cavity options and variants considered in the study are noted in Table 4.4.1–1. The major classes of protection include gas, thin liquid films, thick liquid jets, and solid granules. In addition, a number of more "exotic" ideas have also been proposed, including a frost first wall (for the LMF), a pool-type reactor (Pulse*Star[11]), and magnetic protection.

Table 4.4.1–1. Main Wall Protection Design Options Considered

1. Granular Solid Protection
   - Centrifugally Rotated (CASCADE)[1]
   - Gravity-Driven
2. Thick Liquid Jet
   - Gravity-Driven (HYLIFE I)[2]
   - Magnetically-Guided (SENRI)[3]
   - Advanced Flow Types (HYLIFE-II)[4,5]
3. Liquid Film
   - HIBALL/INPORT,[6] LIBRA[7,8]
   - Porous Composite Wall
4. Gas or Magnetic Protection
   - SOLASE[9]
   - SIRIUS[10]

Granular Solid Protection – An example of a granular solid protection scheme is the one proposed for the CASCADE[1] concept. It consists of a three-layered flowing blanket of pyrolytic carbon, BeO, and solid breeder ceramic (such as $LiAlO_2$) granules. Here, the flowing granules provide both protection and blanket functions. The reactor rotates about its horizontal axis and the moving granule blanket is held against the reactor wall by centrifugal force. The granules are fed by gravity and the rate of flow is controlled by the rotation speed. This concept has attractive safety, efficiency, and low-activation features. Issues are linked to the discontinuity of the heating rate at the BeO/solid breeder interface and to possible aggregation of the granules.

Liquid Protection – Liquid protection schemes use liquid metals or Flibe in the form of either a liquid metal spray, a thick liquid metal wall, or a hybrid concept using a porous solid wall with liquid metal film. Advantages of a spray include the potential uniformity of protection afforded by the mist and the shorter renewal time, while a key issue relates to the stability of the spray formation.

A thick liquid wall was investigated in the HYLIFE-I [2] design study. The concept consists of a liquid lithium waterfall surrounding the micro-explosion area. The lithium fall protects the first wall from the photon and ion fluxes and attenuates the neutron flux so that wall damage is considerably reduced. In this case, the flowing liquid metal provides functions of protection but also of tritium breeding and energy removal. This concept offers advantages in tritium breeding and energy multiplication. However, because of the time necessary to replenish the waterfall, it is mostly suitable for low repetition rate systems. Issues include the effect of the impact on the first wall of liquid lithium slugs propelled by the pressure of lithium vapor created during the micro-explosion. A possible way to alleviate this problem is to use an array of individual jets which could reduce this lithium gas pressure driving force. HYLIFE-II [4,5] continued the concept of a thick liquid jet, but replaced Li with Flibe as the protectant.

An interesting variation for this concept is the use of a magnetic field to guide and stabilize the liquid lithium flow and control flow velocity, as in the SENRI design.[3] The benefit of flow control must be evaluated against the added design complexity resulting from the introduction of magnetic fields.

Another variation of the liquid protection concept is the hybrid (solid/liquid) design, where the falling liquid metal is enclosed in porous solids to prevent disassembly of the liquid following each micro-explosion. For example, in the INPORT modules used in the LIBRA[7,8] and HIBALL[6] design studies, the LiPb columns are made to flow inside porous SiC sleeves. A source of uncertainty is the design and lifetime of these sleeves.

Gas Protection – Gas protection schemes, such as the one used for the SOLASE design,[9] involve filling the reactor cavity with a buffer gas to attenuate the charged particles and soft x-rays before they reach the first wall. Neon is an attractive buffer

gas because of its relatively high stopping power for ions and x-rays and its inertness. Issues include energy re-radiation from the gas to the first wall and its time scale and the effect of impurities and gas breakdown on target performance. The blanket heat removal and tritium breeding function are then carried out separately from the wall protection function. For example, in SOLASE[1], a flow of Li_2O solid breeder particles behind the first wall is used for these functions.

4.4.1.2 Evaluation Criteria - The choice of a cavity wall protection design concept reflects concern over a large number of competing factors. The protection scheme chosen for Prometheus uses a thin liquid Pb film supplied through a porous structure of SiC composite material. The more important concerns which were considered in choosing a thin film protection scheme include:

(1) Configurational Compatibility (Beam Line Accommodation) – Granular and thick film schemes appear nearly impossible to engineer when there are a large number of beam lines. Thick falling films must be guided around all penetrations, without sacrificing protection at any point. We assume that any spot which is not fully covered is likely to be destroyed, such that the protection scheme should be reliable and "passively stable". The beam lines themselves should be protected beyond the first wall, as a significant amount of energy may be deposited there as well. The porous structure could easily be extended into the beam lines.

(2) Engineering Simplicity – One of the unattractive features of a thick falling film is the coupling of functions, including wall protection, breeding, energy conversion, and shielding. While removing components may appear to simplify the design, there are serious disadvantages. The design window is reduced whenever multiple constraints are imposed on a single system. Much of the existing blanket technology from MFE can be applied if a separate blanket is used.

In addition, the technical feasibility of flowing large quantities of liquid at high velocity over large path lengths (and in some cases complex flow schemes) is questionable, especially considering the requirements for beam propagation. There are geometric advantages of a thin film fed from behind the first wall. The flow rate of the film can be very small in comparison.

(3) Safety and Environmental Attractiveness (Minimum Liquid Inventory) – Contamination of the protective film will be very difficult if the inventory is large and, consequently, the required purity level is low. In addition, the reduction in inventory and thickness allows us to choose from a larger number of liquids for the protective medium.

(4) Cavity Clearing – Compared with thick liquid jets, thin films should have better repetition rates. The amount of liquid which can be ejected is limited, and the presence of the porous backing should help contain the film.

(5) Lifetime – The choice of SiC for the structural material has good radiation resistance and safety and environmental advantages. The protective film material can be selected based in part on minimizing radioactivity. In addition, the relatively thick independent first wall system coolant protects the blanket, thus increasing the blanket lifetime.

(6) Versatility – This configuration should be applicable for both HI and laser, for both direct- and indirect-drive schemes.

Gas-protected "dry-wall" concepts, such as SOLASE and SIRIUS, have many desirable features as well, offering good accommodation of beam penetrations, flexibility, and probably the best cavity clearing capability. However, these designs suffer from several problems of their own. Problems arise from the high required gas pressure, including laser-induced gas breakdown and target penetration. Other problems include long energy re-radiation time of the gas and damping of the mechanical impulse from the blast. From past studies, the cavity diameter is likely to be much larger than liquid-protected designs, implying several times as much material and consequently higher cost.

4.4.1.3 Wall Protection Design Choices – The protection scheme chosen for Prometheus uses a thin liquid Pb film supplied through a porous structure of SiC composite material. The SiC structure must be flexible enough to withstand cyclic loading from the blast, but strong enough to support itself and the internal pressure of the film. A supply region behind the porous structure serves to slowly feed the liquid and to remove the heat from the first wall (40% of the total fusion power). Blast energy is removed from the cavity initially by evaporation. During the recondensation phase of each pulse, heat is conducted through the relatively thin film and into the first wall coolant.

The film material is Pb, which offers many advantages:

(1) Appropriate Temperature Ranges – Pb has excellent saturation temperatures in the pressure range of interest (1 mtorr ~ 100 torr). It is high enough for good conduction heat transfer from the film surface to the coolant, but not too high for limits on material properties and compatibility. It is also high enough to provide a high coolant temperature, resulting in good thermal conversion efficiency.
(2) High Thermal Conductivity
(3) Good Neutron Multiplier - Pb is an adequate neutron multiplier which allows elimination of Be in blanket.

(4) Safety Advantages - Since the film contains no Li, the chemical reaction hazard and mobility of Li and LiPb is not a problem.
(5) Chemical Compatibility with SiC
(6) Good Fit with Pb in Hohlraum Targets - Since Pb has been selected as the main high-Z component in the indirect-drive hohlraum targets, impurity control in the liquid is easier.

The main disadvantages of Pb are its weight, low tritium solubility leading to higher permeation, radioactivity (which can be reduced with impurity control), health hazard of Pb vapor, and lower energy multiplication as compared with a Be multiplier.

Having rejected Li and LiPb protectants for safety reasons, Flibe (Li_2BeF_4) was considered as an alternative. Flibe has been extensively studied in the HYLIFE-II[5] reactor studies. While it offers some potential advantages, several concerns led us to select Pb. These areas of concern for Flibe include:

- Poor thermal conductivity (0.8 vs. 34 W/m-K for Pb)
- Dissociation
- Coolant chemistry
- Short-term activation of fluorine
- Chemical reactivity of fluorine
- Mobility of Be and F in vapor form (transport into vacuum system)

The overall configuration of Prometheus is a low aspect ratio cylinder with hemispherical end caps. This configuration was selected for several reasons:

(1) Maintenance of a cylinder is easier than a sphere. Maintenance paths are all straight vertical. The configuration allows independent removal of first wall panels and blanket modules.
(2) A cylinder provides better control of film flow. Problems protecting the upper hemisphere can be reduced with higher aspect ratio, in which the distance from the blast to the upper end cap can be maximized.
(3) A cylindrical configuration is more consistent with conventional plant layouts.

The main disadvantage of this concept is nonuniform power distribution and higher peak loads. The higher peak-to-average loading leads to larger size and higher cost for a given total reactor power. To minimize these disadvantages, the aspect ratio is kept relatively low—of the order of 1-2; however, this also limits the advantage of upper end cap protection.

Another main feature of the Prometheus design is the separate blanket region. This blanket is protected from the blast and is designed to optimize breeding, energy conversion, reliability, and maintainability. A more detailed explanation of the blanket is found in the following section.

The concept described above can be applied to both laser and heavy ion reactor designs. This feature is important in reducing the R&D required for cavity development.

4.4.2 Blanket Concept – The design of the Prometheus blanket was strongly influenced by the desire to maximize safety and reliability. Safety considerations led to the choice of a helium coolant, low-activation solid breeder, and SiC for the structure and neutron reflector. Higher reliability is sought by a combination of vertical maintenance with easily-detachable blanket modules, low coolant pressure with double containment, and relatively conventional configuration adapted from magnetic fusion reactors.

The overall configuration consists of several rings, each containing a number of modules. The modules are configured into the rings outside of the reactor. If any module requires replacement, the entire ring can be removed easily, and then repairs are made to individual modules externally. The module is composed of layers of coolant and breeder. The pressurized He coolant is contained in U-bend woven SiC tube shells. The Li_2O breeder is placed in packed-bed form between the tube shells and is purged by He flowing along the axis of the module.

The Li_2O breeder has many attractive features, including low activation, good temperature window, low tritium inventory, and good existing data base. Of the candidate solid breeder materials, it has the best TBR and, in conjunction with the first wall Pb coolant, provides the potential for adequate tritium breeding without the need for Be as a multiplier.

He coolant also has many advantages. It is chemically inert and can operate at high temperature. This allows high thermal cycle efficiency, but also eliminates the need for a thermal resistance region between the breeder and coolant (all solid breeder materials must operate at high temperature to release their tritium).

In previous blanket design studies, the disadvantages of using He at high pressure have been assessed. These include high pressure stresses, possibly leading to failures, and the fear of leakage problems. In order to reduce these concerns, we took advantage of the unique possibility for low-pressure operation in our design. Inertial fusion inherently produces less neutron power than magnetic fusion. In the Prometheus design, the thick first wall system substantially moderates the neutrons and further reduces the neutron power to the blanket. Only 60% of the thermal power is in the blanket system. Because of the low power density in the Prometheus blanket, the coolant pressure was reduced from the more traditional 5 MPa to only 1.5 MPa. The pressure is so low that the breeder module walls and purge system were designed to withstand coolant tube rupture, resulting in a much higher reliability than higher-pressure designs.

The major penalty paid for this pressure reduction is higher pumping power, resulting in lower thermal cycle efficiency. In this design, the tradeoff was judged favorably for the low pressure design.

Finally, the Pb FW coolant is the sole multiplier. Eliminating Be from the blanket makes the blanket design simpler and also avoids the well-known problems of resource limitations and high cost. Overall, the Prometheus blanket is a very simple and conventional blanket design, yet offers excellent safety, environmental, reliability, and lifetime characteristics.

References for 4.4

1. J. H. Pitts, "Development of the CASCADE Inertial-Confinement Fusion Reactor," Fusion Technology, Vol. 8, No. 1, Part 2B, p. 1198, July 1985.
2. J. A. Blink, et al., "The High-Yield Lithium-Injection Fusion-Energy (HYLIFE) Reactor," UCRL-53559, LLNL, Livermore, December 1985.
3. C. Yamanaka, et al., "Concept and Design of ICF Reactor -SENRI-I," Institute of Laser Engineering Report ILE-8127 P (1981).
4. R. W. Moir, "A Review of Inertial Confinement Fusion (ICF), ICF Reactors, and the HYLIFE-II Concept Using Liquid FLiBe," UCID-21748, 25 September 1989.
5. R. W. Moir, "HYLIFE-II Inertial Confinement Fusion Reactor Design," Fusion Tech. 19 617–624 (May 1991).
6. B. Badger, et al., "HIBALL - A Conceptual Heavy Ion Beam Driven Fusion Reactor Study," UWFDM-450, Fusion Engineering Program, University of Wisconsin (1981).
7. G. A. Moses, et al., "Overview of LIBRA Light Ion Beam Fusion Conceptual Design", Fusion Technology, Vol. 15, No. 2, Part 2A 756, (1989).
8. M. E. Sawan, et al., "Chamber Design for the LIBRA Light Ion Beam Fusion Reactor," Fusion Technology, Vol. 15, No. 2, Part 2A 766, (1989).
9. R. W. Conn, et al., "SOLASE - A Conceptual Laser Fusion Reactor Design," UWFDM-220, University of Wisconsin, December 1977.
10. S. I. Abdel-Khalik, et al., "SIRIUS-M: A Symmetric Illumination, Inertially Confined Direct Drive Materials Test Facility," 2nd Int. Conf. on Fusion Reactor Mater., April 1986.
11. J. A. Blink and W. J. Logan, "The Pulse*Star Inertial Confinement Fusion Reactor", Fusion Technology, Vol. 8, July 1985.

4.5 Selection Criteria for SiC/SiC Composites

4.5.1 Introduction – An important feature of fusion reactions is that the resulting radioactive products are short-lived. However, the interaction of neutrons with structural materials in fusion power systems can lead to long-lived radioactive decay chains. Proper selection of structural materials can lead to significant reductions in the level and duration of environmentally hazardous radioactive products. Several neutronic and conceptual fusion-reactor studies have concluded that the post-shutdown radioactive inventories of FW/B structures made of pure SiC are dramatically lower than any metallic alloy considered for fusion so far.[1-4] The same assessments have shown conclusively that decay heat generated in the reactor, in case of a loss of coolant accident, can be safely and passively removed without the danger of radioactivity release to the environment. It is also realized that long-term radioactive inventories will be mainly controlled by the level of impurities in the structure. Therefore, processing technologies which offer the potential for significant reductions in the level of impurities should be attractive for the development of SiC structures.

Another important feature of SiC structural materials is their high temperature capabilities. Operational temperatures approaching 1000°C are potentially attainable, which can lead to improved thermal cycle efficiency. For these important reasons, the development of SiC structural components is perceived to be of paramount significance to the successful commercialization of fusion energy. This section analyzes and reviews the body of knowledge which is relevant to the application of SiC as a structural material in the inertial confinement reactor concept Prometheus. The relevant features and data base of SiC/SiC composites are presented. On the basis of the available data base and reasonable extrapolations, selection criteria are developed.

4.5.2 Processing of SiC/SiC FRC's - Several methods have been developed for production of SiC fibers for use as reinforcements in high-temperature composites. Continuous yarns of 500 fibers are now in commercial production by Nippon Carbon Company[1] under the trade name Nicalon. The process starts by dechlorinating dichlorodimethylsilane with molten metallic sodium to produce the solid polymer. Further processing steps are polymerization, and densification of amorphous Si and C at high temperatures (1200°C-1500°C). The final microstructure is crystalline β-SiC of density in the range 3.16 g/cm^3, and of crystallite size of 20-50 μm. The final product is continuous multifilament tows comprised of 500 filaments.

SiC monofilaments can also be prepared by the chemical vapor deposition (CVD) process, as described in References 2 and 3. SiC is deposited from vapor mixtures of alkyl silanes and H_2 onto a substrate formed by a resistance-heated W wire or C filament. The substrate has a diameter of 10-25 μm and forms the fiber core. The final

filament is commonly 100-150 μm in diameter. Although deposition at high temperatures (above 1300°C) is fast, the resulting structure is coarse crystalline and is weaker than the amorphous structure obtained at lower temperatures. If any free silicon appears in the microstructure, further weakening will result.

Whiskers of SiC can be prepared either from rice hulls[4] or by a vapor-liquid-solid (VLS) process.[5] Rice hull whiskers contain around 10% SiO_2 and between 0%-10% Si_3N_4. Around 10% of SiC is in the β crystalline phase, and the remainder is composed of α-SiC particulates. Whiskers produced from rice hulls are short, with lengths around 50 μm. Longer and smoother whiskers are prepared at Los Alamos[5] by the VLS process. Such whiskers possess superb mechanical properties, with an average strength of 8.4 GPa and an average elastic modulus of 580 GPa.

Multifilament fibers can be assembled into two- and three-dimensional structures by interlacing, intertwining, or interlooping. Combining the high strength of fibers with proper matrix-fiber interface frictional properties, fiber architectures will expand the design options for tough and reliable fusion structural materials. Fiber architectures can be classified into four categories: discrete, continuous, two-dimensional, and fully integrated (three-dimensional). Selection of one of these architectures for F/B or high heat flux applications will depend on a number of factors. These are: (1) the capability for in-plane multi-axial reinforcements, (2) through-thickness reinforcements, (3) the capability for final shape manufacturing, and (4) leak-tightness of the final components during high-temperature operation. Selection of a particular form of architecture for fusion may be premature at present, because matrix processing techniques are still evolving. While 3-D architectures provide an orthotropically tougher composite, the CVI technology employed at present is limited to low fiber volume fractions, and the procedure is quite lengthy. On the other hand, 2-D laminates can be produced at much greater speeds and can achieve higher fiber volume fractions. The final component mechanical properties will be anisotropic. This feature will certainly lead to reduced capabilities of components to carry shear loads. In summary, processing technologies for the manufacture of SiC/SiC FRM's are available at present. However, further development is needed for production of components on a commercial scale.

4.5.3 Data Base - SiC is known to have high intrinsic strength and stiffness (E = 450 GPa at RT), high-temperature stability (decomposition temperature = 2830°C), and excellent oxidation resistance. Its relatively high conductivity ($k = 0.25$ W cm^{-1} $°C^{-1}$ at 200°C) and low coefficient of thermal expansion ($\alpha = 3.8 \times 10^{-6}$ $°C^{-1}$ at 200°C) results in favorable thermal shock resistance when compared to other ceramic materials. The thermal conductivity of CVD SiC, k(W cm^{-1} $°C^{-1}$), and the specific heat, C_p (J Kg^{-1} $°C^{-1}$), are given by empirical equations of the form:

$$\text{Property} = \sum_{i=1}^{4} M_i T^j$$

where T is temperature in °C. Values of the polynomial fit coefficients are shown in Table 4.5.3-1. Graphical representation of these properties as functions of temperature is shown in Figure 4.5.3-1.

Table 4.5.3-1. Coefficients of Polynomial Fits to Selected Properties of SiC

$$\text{Property} = \sum_{i=1}^{4} M_i T^j$$

Property Coefficient	Thermal Conductivity $W\,m^{-1}\,K^{-1}$	Specific Heat $J\,Kg^{-1}\,K^{-1}$	Fracture Stress, σ_f MPa	Young's Modulus GPa	Swelling δV/V <1000°C	Swelling δV/V >1000°C
M_0	62.84	435.53	−993.9	605.632	1.43	−71.19
M_1	−0.04	3.08	7.42	−1.407	0.0059	0.15
M_2	6.25×10^{-6}	−0.0047	−0.013	0.003	-1.56×10^{-9}	1.09×10^{-4}
M_3	0	3.31×10^{-6}	9.54×10^{-6}	-2.087×10^{-6}	8.58×10^{-9}	2.56×10^{-8}
M_4	0	-8.41×10^{-10}	-2.42×10^{-9}	0	0	0

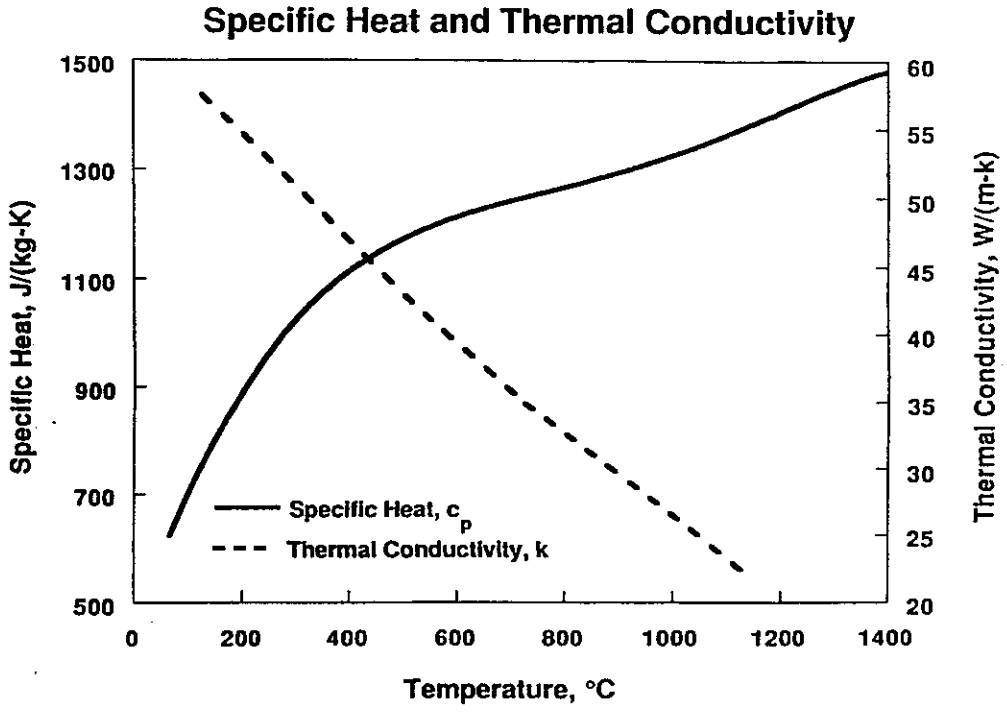

Figure 4.5.3-1. Dependence of the Specific Heat and Thermal Conductivity of SiC on Temperature

Assessment of the data base and development of a proper fusion-specific SiC composite is an iterative process. For this reason, we discuss here the available mechanical and radiation effects data base so that ways for further improvements can be found.

4.5.3.1 Mechanical Properties – The tensile strength of Nicalon fibers is statistical because of the existence of defects (e.g. voids and cracks) during the manufacturing process. It is also strongly influenced by heat treatment, test atmosphere, and test temperature. Commercial Nicalon fibers in various atmospheres show degradation in strength at or above 1000°C.[6] Strength deterioration is attributed to: (1) chemical reaction between SiO_2 and free C, leading to surface damage; (2) crystallization of the amorphous structure; and (3) oxidation in gaseous atmospheres. The tensile strength of CVD-prepared SiC fibers on C cores is retained only up to 800°C. The 100 h rupture strength of CVD fibers was shown to degrade greatly above 1100°C.[7] While the average tensile strength of unirradiated monofilaments is 2.8 GPa at temperatures below 900°C, preform wires have an average flexural strength of only 1.3 GPa. The uniform elongation at fracture is 1.5-2.0%.

For CVD fibers, it was observed that fiber creep is anelastic (i.e. recoverable) and is a result of grain boundary sliding,[8] controlled mainly by a small amount of free silicon in the grain boundary. Fiber creep activation energy of 480 kJ $mole^{-1}$ was concluded to be similar to sintered SiC material, and the resulting creep rate is about an order of magnitude greater than the Nicalon fibers.[8] The lower creep resistance of the more commercial Nicalon fibers was attributed to the lower grain boundary (GB) viscosity of free Si, which results from the polymerization process. Diffusional creep by GB sliding has an activation energy estimated at 611 kJ $mole^{-1}$ and a pre-exponential of 3.1×10^{-7} m^2 s^{-1}.[Ref.9]

These observations indicate that high-temperature creep properties of the composite may be life-limiting in fusion. In particular, the crack bridging mechanism, which is the main feature for enhancement of the composite's toughness, will have to be critically examined since the bridging fibers may creep at a faster rate than the matrix itself.

The high-temperature deformation characteristics of hot-pressed SiC have been experimentally investigated and may be taken as indicative of the matrix in a composite.[8,9] The activation energies for power law as well as lattice diffusion creep were found to be about 912 kJ $mole^{-1}$.[Ref.9] Transition from power law creep at high stresses to diffusional creep at low stresses was also observed.[10] However, the diffusional matrix creep rates were found to be very small. A power law index of 5 was found to be similar to that of pure Si. The mechanical properties of unirradiated reaction sintered SiC (i.e., Young's modulus, E (GPa), and bend strength, σ_f (MPa)) as

functions of temperature, T (°C), are also given by polynomial fits, with coefficients defined in Table 4.5.3-1. Graphical representation is shown in Figure 4.5.3-2.

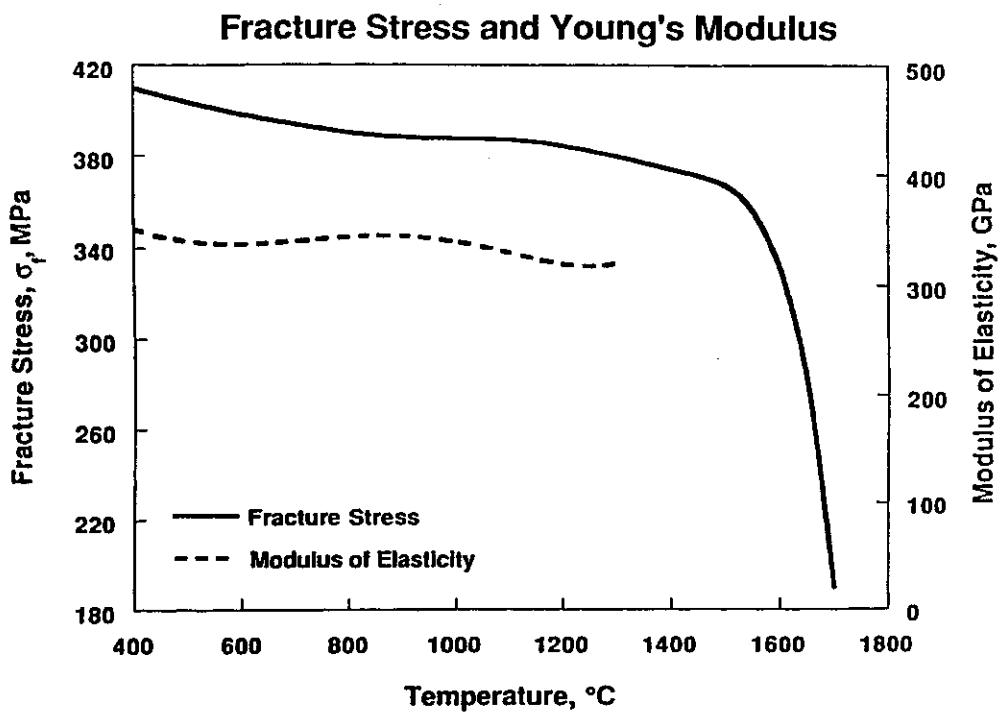

Figure 4.5.3-2. Temperature Dependence of the Fracture Stress and Young's Modulus of SiC

The critical stress intensity factor of the SiC matrix is expected to be low, as compared to metallic alloys. However, the bridging of cracks with the strong fibers will possibly allow for higher values of an apparent K_{IC}, especially when one is concerned about catastrophic through cracks. Room temperature values of K_{IC} for an unbridged hot pressed SiC range from 2.6 to 5.7 $MN.M^{-3/2}$ and is independent of temperature up to 1000°C. Sintered SiC shows temperature-independent K_{IC} of about 3 $MN.M^{-3/2}$ up to 1500°C.

An allowable design stress for SiC FRC's will depend on a wide range of manufacturing and operational factors. For example, recent fracture test results at PNL at 800°C on SiC FRM's from several vendors showed them to have strengths in the range 300-600 MPa in the unirradiated condition. Neutron irradiation at the same temperature, and up to approximately 10 dpa, showed that the fracture strength declined by about a factor of 2–2.5.[11] It is possible then, with modest technology extrapolation, that low pressure FW/B components would be designed to operate reliably in a fusion environment.

4.5.3.2 Coolant Compatibility – SiC has excellent resistance to oxidation up to 1000°C, because of the formation of a protective stable SiO_2 layer. Rapid oxidation may occur, however, depending on the physical state of the oxide layer between 100°C and 1300°C. The porous oxide layer offers no resistance to the diffusion of oxygen to react with the SiC forming volatile Si and C oxides. The stability of the SiO_2 layer is dependent on the O_2 partial pressure, being unstable at pressures lower than 10^{-10} to 10^{-8} atmospheres.[12] In a primary helium loop, the partial pressure of O_2 is expected to exceed these values. However, the reaction of the interfacial layer between the fibers and the matrix with oxygen will ultimately determine the upper usable temperature of the composite, as far as compatibility is concerned. At present, this layer is either C, BC_4, or BN. While carbon oxidation will severely limit the upper temperature, the production of He and H from nuclear reactions in B compounds is expected to degrade the strength of SiC FRC's. An important factor which needs yet to be studied is the possible reduction of the passive SiO_2 layer by tritium or hydrogen.

Compatibility studies of SiC in molten Li indicated that intergranular penetration degrades its fracture strength.[13] Reaction with the glassy phase at the GB is thought to be the cause of this rapid penetration. In a molten lithium environment, the uniform corrosion rate was reported to be extensive.[13] However, the reported data was obtained at O_2 activities thought to be much higher than anticipated in a typical Li loop of a fusion reactor.[11]

4.5.3.3 Radiation Effects – The strong directional bonding and the mass difference between Si and C atoms render the crystalline form of β-SiC exceptional radiation resistance characteristics. Recent Molecular Dynamics (MD) studies[14] show that Replacement Collision Sequences (RCS's) are improbable, and that the displacement of C atoms is much easier than Si. MD computer simulations[14] show that while the average threshold displacement energy (E_d) is 15 eV for C, it is about 90 eV for Si. This result would directly lead to the conclusion that the stoichiometry of the displacement cascade will differ substantially from that of the matrix. It is also observed that energetic Si PKA's displace multiple C atoms which end up on <111> planes. Thus, C-rich interstitial dislocation loops will tend to form on <111> planes. Experimental observations at temperatures below 1000°C tend to corroborate this conclusion.[15] Vacancies and He atoms exhibit considerable mobility above 1000°C. These fundamental considerations may explain some of the observed features of SiC dimensional changes as a function of temperature and fluence.[15-18]

The ease by which C atoms can be displaced, as compared to Si, would indicate that C-rich interstitial loops may tend to be prevalent as a result of irradiation. Energetic Si atoms traveling the <111> gap induce simultaneous displacements of multiple C atoms on {111} planes. Price[15] observed Frank-type loops on {111} planes which may be C-rich. Below 1000°C, point defects tend to form loops on {111} planes and swelling is therefore expected to saturate. For example, Harrison and Correli[19] observed large loops (10-200 nm) in RB-SiC after neutron irradiation to a fluence of

1.8×10^{23} cm^{-2}. At temperatures above 1000°C, cavities form and swelling does not saturate. The presence of helium results in further increases in the swelling rate by the known gas-driven swelling mechanism, as observed in the swelling of nuclear fuels. Swelling data with helium generation are scarce and need future considerations. Swelling of β-SiC in the temperature range 625-1500°C and at a neutron fluence (E > 0.18 MeV) of 1.2×10^{22} [Ref.15] is represented by two separate polynomials, with two different sets of coefficients below and above 1000°C, respectively. The coefficients and the general swelling behavior as a function of temperature is shown in Figure 4.5.3-3. Additional helium will drive swelling to higher values, particularly at temperatures above 1200°C.[20]

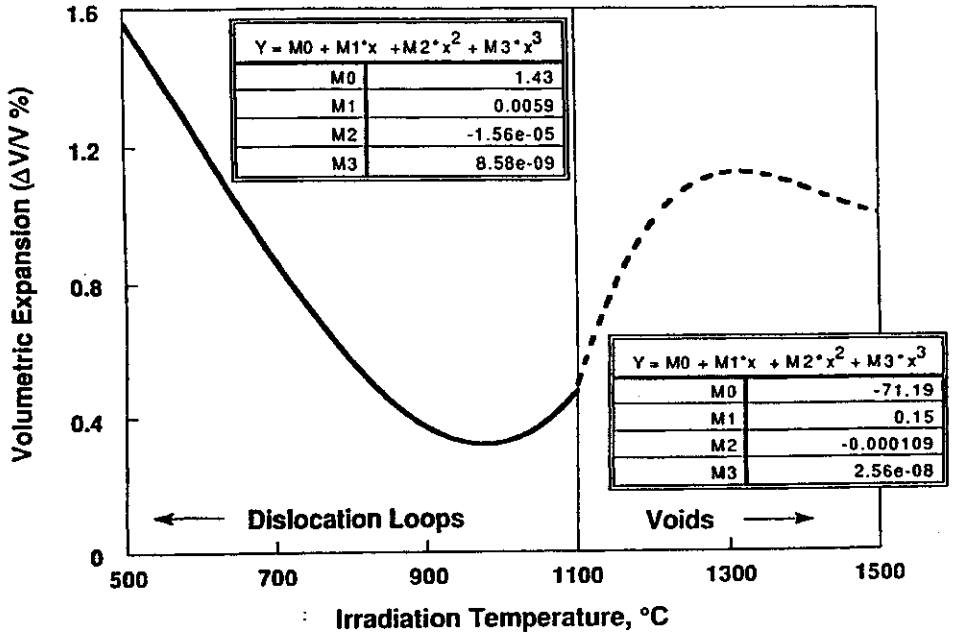

Figure 4.5.3-3. Volumetric Swelling of SiC as a Function of Temperature at a Neutron Fluence of 1.2×10^{22} n cm^{-2} (E>0.18 MeV)

A significant irradiation damage problem which results in the deterioration of the mechanical properties of SiC is the crystalline-to-amorphous phase transition phenomenon. For example, the strength of Nicalon fibers is degraded by irradiation-induced re-crystallization. Crystallites growing out of the fibers into the matrix form nucleation sites for cracks leading to delamination of the interface. The limited accumulated evidence from radiation effects data indicate that the upper temperature limit for use of SiC in structural design is in the range of 900-1000°C.

4.5.4 Design With SiC/SiC Composites – Design rules for SiC/SiC composites in the high-temperature and radiation environment of fusion reactors are obviously not established, mainly because the test data base is not complete. This data base for mechanical properties must also be made on full-size components. It is interesting to note that the fracture behavior of the composite is totally different from monolithic

behavior, and exhibits considerable apparent ductility, as shown in Figure 4.5.4-1. However, this increased toughness is caused by the dissipation of the elastic energy in slow micro-cracking processes. Failure stresses will have to be determined for particular applications (e.g. load bearing but not leak-tight components, leak-tight components, components which resist thermal stresses, etc.). A promising failure approach would be to use an interactive theory, such as the Tsa-Wu criterion. In such an approach, the failure stress tensor is measured. This would give failure stress

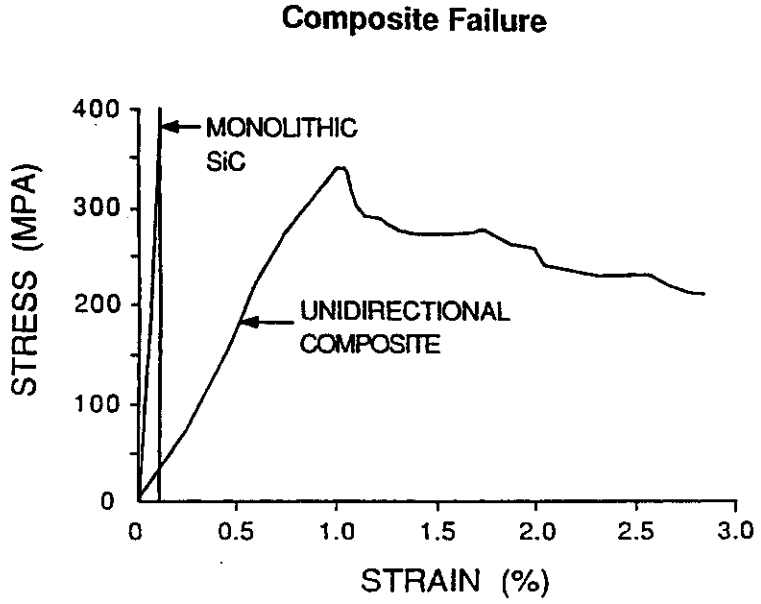

Figure 4.5.4-1. Stress-Strain Behavior of Monolithic and Unidirectional Composite SiC at Room Temperature

components in tension, compression, and shear, for both in-plane and out-of-plane components. Structural analysis would be fairly complete and would result in the definition of safety factors in each direction. This approach would take into account the probabilistic variability of properties, as determined by experimental measurements. There will be no need to use Weibull statistical analysis because safety factors and the experimental failure tensor would guarantee safe operation, as desired, from a particular component.

4.5.5 Selection Rationale – SiC/SiC FRC's are excellent, low-activation, safe structural materials for the high-temperature and radiation environment in commercial fusion reactors. Their superior mechanical and physical properties would allow for operational temperatures approaching 900–1000°C, thus achieving high thermal cycle efficiencies. The strong covalent bond between Si and C results in promising resistance to the damaging effects of neutron irradiation. Increased toughness because of the reinforcement with strong fibers will make deterministic design

approaches possible. However, considerable research and development will be needed before the material will be able to meet its promise.

References for Section 4.5

1. S. Yajima, K. Okamura, J. Hayashi and M. Omori, J. Amer. Ceram. Soc., 59 (1976) 324.
2. E. Fitzer, D. Kehr, and M. Shahibkar, in: Silicon Carbide-1973, Marshal, Faust and Ryan, Eds. (Univ. of South Carolina Press, USA, 1974) p33.
3. H. E. DeBolt, V. J. Krukonis, and F. E. Wawne, in: ibid., p.168.
4. I. B. Cutler, "Production of SiC from Rice Hulls," U.S. Patent # 3,754,076, 1976.
5. G. Hurtley and J. Petrovic, in: Proc. Adv. Composites Conf., M. W. Liedtke and W. H. Todd, Eds., ASM, 1985, p.401.
6. S. Yajima, H. Kayaro, K. Okamura, M. Omori, J. Hayashi, T. Matsuzwa, and K. Akutsu, Am. Chem. Soc. Bull., 55 (1976) 1065.
7. I. Ahmad, D. N. Hill, and W. Hefferman, in: Proc. Inter. Conf. Comp. Mater., AIME, 1976, vol 1, p. 85.
8. J. Decarlo, J. Mater. Sci., 21 (1986) 217.
9. P.M. Sargent and M. F. Ashby, Scripta Met., 17 (1983) 951.
10. A. Djemel, J. Cadoz and J. Philibert , in: Creep and Fracture of Engineering materials and Structures, B. Wilshire and D. R. J. Owen, Eds., Pineridge, Swansea, U.K., 1981, p. 381.
11. R. H. Jones, in: Fusion Reactor Materials Semiannual Progress Report, March 1991, DOE/ER-0313/10, p. 215.
12. E. A Gulbransen and S. A. Jansson, Oxid. Met., 4 (1972) 181.
13. D. R. Curran and M. F. Amateau, Amer. Cer. Soc. Bull., 65 (1986) 1419.
14. A. Elazab and N. M. Ghoniem, ICFRM-5.
15. R. J. Price, J. Nucl. Mater., 46(1973)268.
16. R. Blackstone and E. H. Voice, J. Nucl. Mater. 39(1971)319.
17. A. M. Carey, F. J. Pineau, C. W. Lee, and J. C. Corelli, J. Nucl. Mater., 103&104(1981)789.
18. K. Hojou and K. Izui, J. Nucl. Mater., 160(1988)334.
19. S. D. Harrison and J. C. Corelli, J. Nucl. Mater., 122&123(1984)833.
20. T. Suzuki and T. Iseki, J. Nucl. Mater., 170(1990)113.